Modeling of Frost Growth on Heat Exchanger Surfaces

Katrin Prölss, Gerhard Schmitz
Hamburg University of Technology, Applied Thermodynamics Group
Denickestr. 17, 21075 Hamburg

Abstract

A Modelica model to study the frost growth on parallel heat exchanger plates is developed. The coupled heat and mass transport phenomena involved in the process are described. A physical model which includes the distributed densification of the frost layer is compared to a simple lumped model approach. The frost structure and thus the resulting properties such as density and thermal conductivity are found to have a strong influence on the model results. Empirical correlations for properties and transport coefficients are used in both models. The model describing the airflow is taken from the *Modelica_Fluid* library and extended to handle condensation and freezing of water vapor. The *Modelica.Media* library provides the moist air property model.

1 Introduction

Frost formation on heat exchanger surfaces in air cooling applications always occurs when the coil surface temperature drops below the freezing point of water and the dew point temperature of the air in contact with the cold surface. The main problems associated with frost growth are the decline in heat exchanger efficiency resulting from an insulating effect of the frost layer and the rising pressure drop due to a decreasing hydraulic diameter of the flow channel, which in return increases the energy consumption of the fan. Usually a system operating under frosting conditions needs a defrost from time to time. In order to estimate the allowable frost growth period and the energy required to melt down the frost layer, its stored amount of frozen water, thickness and thermal behavior have to be known. Several studies exist which try to formulate empirical approaches to predict the behavior of certain types of heat exchangers and surfaces, see e.g. [1], [2]. Hoffenbecker *et al.* [3] investigated defrost cycles with fin-and-tube heat exchangers and developed a numerical model describing the process with given initial frost conditions. Over the past decades several attempts have been made to develop physical models of the transport phenomena which govern the general formation of a frost layer. In 1974 Sanders [4] already proposed a system of partial differential equations describing the coupled heat and mass transport processes in his detailed study on frost structure and provided several simplified approaches. Le Gall *et al.* [5] and Tao *et al.* [6] developed more detailed models and focused on the diffusion process of water vapor through the porous medium. But due to the complex structure and variety of ice crystal formation an entirely physical approach is hardly possible and the quality of the model still relies on some empirical correlations.

The transport phenomena involved in the frost formation process are sketched in figure 1. Warm moist air

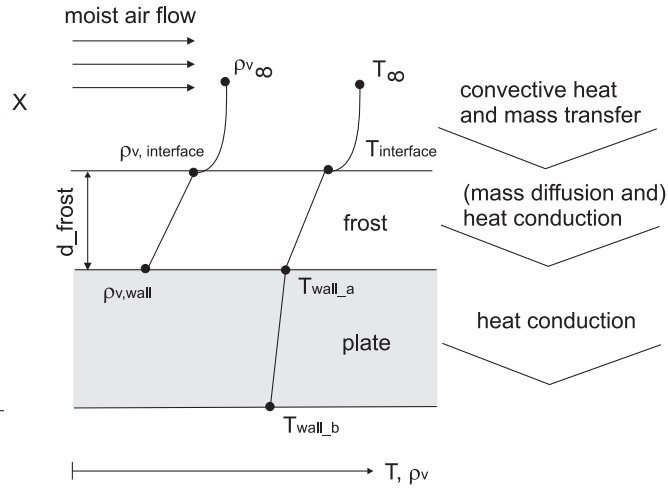

Figure 1: Transport phenomena in a porous frost layer

passes a cold surface with a temperature below the freezing point of water and the dew point of the air. Heat transfer by forced convection occurs from the bulk flow to the cryosurface, driven by a temperature gradient. A concentration gradient causes a water vapor flux from the bulk flow to the frost surface where part of it freezes and adds to an increase of the layer while releasing latent heat. Part of the water vapor dif-

fuses into the frost layer leading to a densification of the structure. The sum of sensible and latent heat is transported to the cold wall interface by thermal conduction.

2 Modeling the frost formation process

2.1 Frost formation types

During the process of frost deposition on a cold surface several stages of frost formation may be distinguished. Hayashi *et al.* [7] found three periods describing the formation of a frost layer:

- the crystal growth period
- the frost layer growth period
- the frost layer full growth period

The first corresponds to the first formation of ice crystals on the cryosurface, which basically form parallel columns or needles growing in one dimension. In the frost layer growth period they start interbranching which leads to a meshed more uniform frost layer. The surface temperature of the frost gradually increases with increased frost thickness due to a rising thermal resistance. When the triple point temperature is reached the frost surface begins to melt, water soaks into the frost and decreases its thermal resistance, which again leads to additional frost deposition and under continuous melting and freezing eventually to a dense and tight layer. This stage is referred to as the full growth period. In the following model only the frost layer growth period will be considered.
Hayashi *et al.* classified four types of frost crystal structure with respect to the cryosurface temperature and the water concentration difference between bulk flow and surface. Generally, higher cryosurface temperatures and lower concentration gradients lead to denser and more homogeneous frost layers. In the same study the frost type was found to have a strong influence on frost properties like density and thermal conductivity.

2.2 Energy and mass balances

Heat and mass transport through the ice layer are considered one-dimensional, because a prevailing temperature gradient and a frost dimension very small compared to the other two is assumed perpendicular to wall and air flow. Further assumptions are that temperature variations of moist air and ice properties are neglected, the total gas phase pressure is constant throughout the porous medium, radiation effects are neglected and thermodynamic equilibrium prevails between ice and air in the pores.
The water mass balance over the ice phase of the frost layer can be written as the change of accumulated ice and water vapor equal to the spatial change of the diffusive vapor transport rate [5].

$$\frac{\partial(\rho_\alpha\,\varepsilon_\alpha)}{\partial t}+\frac{\partial(\rho_{\mathrm{v,sat}}\,\varepsilon_\beta)}{\partial t}=-\frac{\partial \dot{m}_\mathrm{v}}{\partial x} \tag{1}$$

where $\dot{m}_\mathrm{v}$ is the water vapor mass flow per unit area and ρ_α is the density of ice. The moist air in the frost pores is always assumed to be saturated with vapor, the vapor density $\rho_{\mathrm{v,sat}}$ in the gas phase is therefore determined by the local temperature applying the ideal gas law and the saturation pressure curve of water. ε_α and ε_β are the ice and moist air volume fractions, respectively. The driving potential for the diffusive water transport is the gradient of vapor partial pressure in the gas phase p_v, the resulting vapor flux for molecular diffusion is then obtained from [8]

$$\dot{m}_\mathrm{v}=-\frac{D_\mathrm{eff}}{R_\mathrm{v}T}\,\frac{\partial p_\mathrm{v}}{\partial x} \tag{2}$$

with D_eff as the effective coefficient of diffusion and R_v as the ideal gas constant of water, T is the local temperature.
Equation 1 may then be transformed into

$$\frac{\partial\,\rho_{\mathrm{v,sat}}}{\partial T}(1-\varepsilon_\alpha)\frac{\partial\,T}{\partial t}+(\rho_\alpha-\rho_{\mathrm{v,sat}})\frac{\partial\,\varepsilon_\alpha}{\partial t} =\frac{\partial}{\partial x}\left(\frac{D_\mathrm{eff}}{R_\mathrm{v}T}\,\frac{\partial p_\mathrm{v}}{\partial x}\right). \tag{3}$$

The energy balance over the frost element is

$$\frac{\partial u_\mathrm{f}^*}{\partial t}=\frac{\partial}{\partial x}\left(\lambda_\mathrm{f}\frac{\partial T}{\partial x}\right)-\frac{\partial \dot{m}_\mathrm{v}}{\partial x}\Delta h_\mathrm{sv} \tag{4}$$

The first term on the right handside of equation 4 corresponds to the conductive heat flow, the second represents the enthalpy tranport associated with the diffusive vapor flux with Δh_sv as the heat of fusion. The frost energy per unit volume u^* is given by

$$u_\mathrm{f}^*=c_\mathrm{f}\,\rho_\mathrm{f}\,T+(1-\varepsilon_\alpha)\,\rho_{\mathrm{v,sat}}\,\Delta h_\mathrm{sv} \tag{5}$$

where c_f is the specific heat capacity of frost, ρ_f is the frost density and T is the local temperature.
A simplifying assumption to the problem is the neglection of water vapor diffusing into the frost layer. The

energy balance then reduces to the basic formulation of unsteady heat conduction [8].

$$\frac{\partial(\rho_f\, c_f\, T)}{\partial\, t} = \frac{\partial}{\partial x}\left(\lambda_f \frac{\partial\, T}{\partial x}\right) \quad (6)$$

2.3 Boundary conditions

2.3.1 Wall

The boundary conditions at the wall side of the frost layer are:

$$\begin{aligned} T(x = x_w) &= T_w \\ \dot{m}_v(x = x_w) &= 0\,. \end{aligned} \quad (7)$$

The index w denotes the position at the wall interface, $\dot{m}_v$ is the water vapor flux.

2.3.2 Airside heat and mass transfer

The heat transferred from the airflow to the frost surface is expressed as the sum of sensible and latent heat flows.

$$\dot{q}_{sens} + \dot{q}_{lat} = \lambda_f(x_s)\,\frac{\partial T_s}{\partial x} \quad (8)$$

$$\alpha(T_b - T_s) + \Delta h_{sv}(\dot{m}_t - \dot{m}_{v,s}) = \lambda_f(x_s)\,\frac{\partial T_s}{\partial x} \quad (9)$$

where α is the coefficient of heat transfer, T_b is the bulk air temperature and the index s denotes surface properties. $\dot{m}_t$ and $\dot{m}_{v,s}$ are the total vapor flux from the air to the frost layer and the vapor flux into the frost layer, respectively. They may be determined from

$$\dot{m}_{v,s} = \dot{m}_v(x = x_s) = \left(\frac{D_{eff}}{R_v T}\right)_s \frac{\partial p_{v,s}}{\partial x} \quad (10)$$

$$\dot{m}_t = \rho_a \beta (X_b - X_s) \quad (11)$$

where β is the mass transfer coefficient in m/s and X is the absolute humidity in in the bulk flow and at the frost surface, respectively and ρ_a is the air density. Substracting the two fluxes yields the frost deposition rate at the frost surface.

$$\rho_{f,s}\frac{\partial x_s}{\partial t} = \dot{m}_t - \dot{m}_{v,s} \quad (12)$$

The surface density may be calculated from an empirical correlation by Hayashi *et al.* [9]

$$\rho_{f,s} = 650\, e^{0.227(T_s - 273.15)} \quad (13)$$

where T_s is the surface temperature in K. In [6] a zero gradient for the ice volume fraction is assumed at the surface.

$$\frac{\partial \varepsilon_{\alpha,s}}{\partial x} = 0; \quad (14)$$

If a simplified model is used that does not account for water diffusion into the frost, $\dot{m}_{v,s}$ is set to zero and the entire water mass flow towards the frost surface is assumed to contribute to the increase of frost layer height.

Empirical correlations are used to determine the transport coefficients. In the literature the Chilton-Colburn analogy between heat and mass transfer seems to be widely accepted also under frosting conditions [2] [11]. It relates the mass transfer coefficient β to the heat transfer coefficient α using the Lewis number Le:

$$\beta = \frac{\alpha}{c_p\, \rho_a} Le^{2/3} \quad (15)$$

ρ_a ist the moist air density and c_p is the specific heat capacity. According to [2] the heat transfer coefficients are normally higher under frosting conditions compared to a smooth surface due to an increased surface roughness. However, it is unclear if the reduction of the hydraulic diameter also adds to this reported increase. The following correlation suggested by [2] for air flow between parallel plates for Reynolds number ranging from 6000 to 50000 was used:

$$Nu_f = 0.034\, Re^{0.8} \quad (16)$$

where the Reynolds number is based on the hydraulic diameter of the parallel plate channel.

2.4 Frost properties

As described above the prediction of frost layer thickness and its thermal behavior largely depends on frost properties such as density, thermal conductivity and the effective diffusion coefficient of water vapor in the air filled porous medium. The diversity of possible frost structures as indicated in section 2.1 clearly shows that an accurate determination of those properties for a wide range of operating conditions and heat exchanger types may be a difficult task. The wide range of empirical correlations and theoretical models that have been established sometimes are mostly applicable only in a very limited operating range. A literature review of empirical correlations for frost properties and frost layer thickness can be found e.g. in [2].

2.4.1 Thermal conductivity

The significant thermal resistance added to the heat exchanger wall by the growing frost layer results from the rather low thermal conductivity of the ice-air composite. The air in the pores largely contributes to the

insulating effect. Also the structure and orientation of the ice crystals influence the material property. There is an agreement in the literature that thermal conductivity is a strong function of frost density with only a weak dependence on temperature. An empirical correlation based on the frost layer density from [10] is used for the proposed models:

$$\lambda_f = 0.02442 + 7.214 \cdot 10^{-4}\rho_f + 1.1797 \cdot 10^{-6}\rho_f^2 \,. \quad (17)$$

Another correlation suggested by [2] is

$$\lambda_f = 1.202 \cdot 10^{-3}\ \rho_f^{0.963} \quad (18)$$

More theoretical approaches take into account the (generally assumed) frost structure and sometimes even the surface roughness as in [11]. All correlations are found between the two ideal assumptions of ice crystals parallel and perpendicular to the prevailing direction of heat transport. The first orientation corresponds to thermal resistances in series, the second to a parallel arrangement. Their conductivities can be obtained as follows

$$\begin{aligned} 1/\lambda_{per} &= (1-\varepsilon_\alpha)/\lambda_a + \varepsilon_\alpha/\lambda_\alpha \ \text{(perpendicular)} \\ \lambda_{par} &= (1-\varepsilon_\alpha)\lambda_a + \varepsilon_\alpha\lambda_\alpha \ \text{(parallel)} \end{aligned} \quad (19)$$

where λ_a and λ_α are the thermal conductivities of air and ice, respectively. A comparison of this approach with eq. (17) and (18) is given in figure 2. It shows that the presented empirical correlations are found within the two ideal structure models, but still reveal significant deviations in one to another. It is expected that differences in frost structure which cannot be related to density or ice volume fraction alone that are caused by variable frost growth conditions and aging effects also play an important role.

2.4.2 Density and specific heat capacity

The way to determine the frost density depends on the assumptions made for the vapor transport in section 2.2. If equation 1 is used, the density distribution in the frost layer can be determined from the ice volume fraction ε_α

$$\begin{aligned} \rho_f &= \varepsilon_\alpha\rho_\alpha + (1-\varepsilon_\alpha)(\rho_a + \rho_v) && (20) \\ &\approx \varepsilon_\alpha\rho_\alpha && (21) \end{aligned}$$

The volumetric heat capacity may be computed in a similar way and with neglection of the gas phase impact reduces to:

$$\rho_f c_f \approx \varepsilon_\alpha\rho_\alpha c_\alpha \quad (22)$$

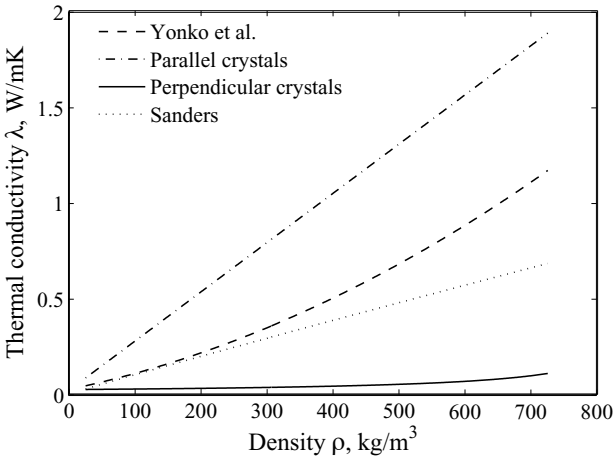

Figure 2: Thermal conductivity vs. frost density for the empirical correlation by Yonko et al. (17), the correlation by Sanders (18) as well as perpendicular and parallel ice crystal orientation, respectively.

If the frost layer is assumed to have a uniform density over the entire frost height and equation 6 is used, the average frost density $\bar{\rho}_f$ is computed from a mass balance over the total frost layer,

$$\frac{\partial(\bar{\rho}_f\delta_f)}{\partial t} = \dot{m}_t \quad (23)$$

with $\dot{m}_t$ from eq. (10) and the frost thickness δ_f.

2.4.3 Coefficient of diffusion

Following from (10) the frost density largely depends on the water vapor that diffuses into the frost layer. The effective diffusion coefficient D_{eff} in (3) accounts for several complex mechanisms. Those involve besides molecular diffusion the tortuosity of the porous frost structure, the variation of pore diameters, phase transitions and others. The effective diffusion coefficient may be expressed in terms of the binary diffusion coefficient D_{AB}

$$D_{eff} = \mu D_{AB} \quad (24)$$

Several works focus on the determination of the μ factor with significantly different results. The first models dealing with effective diffusion factors for frost always assumed lower values than those for molecular diffusion ($\mu \leq 1$), others including Tao *et al.* in [6] report values several times larger. Le Gall *et al.* propose a correlation that combines both approaches and try to determine the factor F in the following equation empirically with respect to selected boundary conditions

[5].

$$\mu = \frac{1-\varepsilon_\alpha}{1-0.58\,\varepsilon_\alpha} + 10\,F\,\varepsilon_\alpha\,(1-\varepsilon_\alpha)^{10} \quad (25)$$

F will also be treated as a constant parameter input to (25) in the distributed model and discussed further below.

3 Implementation of the model in Modelica

A Modelica model is developed to investigate the impact of frost growth on parallel plates passed by a moist airflow. A model structure that allows a flexible and easy change of the level of detail and used correlations is aimed for.
The transport phenomena involved can be divided into groups with respect to their location in the combined problem.

- heat and mass transport by forced convection - spatial resolution in air flow direction required
- heat and mass transport through thermal and concentration boundary layers - transport phenomena are lumped by using transport coefficients from empirical correlations
- conductive heat and diffusive mass transport through the frost layer - spatial resolution perpendicular to airflow direction required
- conductive heat transport through the solid wall - spatial resolution perpendicular to airflow required

The first two are combined in an air flow model partly taken from the Modelica_Fluid library, frost layer and wall are combined in a second component for the reasons specified further below.

3.1 Airflow model

The model that describes the moist airflow in a a channel formed by two flat plates is extended from the base class `PartialDistributedFlow` in the *Modelica_Fluid* library. Conservation of energy, total mass, substance mass and momentum as well as flow reversal are handled in this model applying a one-dimensional finite volume approach with upwind discretization. The medium model for moist air was taken from the *Modelica.Media* library. The energy and mass balances contain source (or sink) terms which can be used to include heat and massflow across the volume boundaries. Those heat and mass flow rates are determined in a replaceable subcomponent `heat` which is added to the extended air model. The total volume and hydraulic diameter depend on the internal dimensions of the flow channel, which may change with an increasing frost layer.

3.2 Wall and frost model

3.2.1 Implemented frost models

Three frost models are implemented in Modelica reflecting different levels of detail.

I Distributed frost densities (ice volume fractions), diffusive vapor transport into frost. Balance equations (3) and (4), boundary conditions (7) - (12,(14) and property calculations (19), (23), (24) and (25) are used.

II Frost density changes only due to temperature dependent surface density during frost deposition. Water vapor diffusion in the frost layer is neglected. Balance equations (6) and (23), boundary conditions (7) - (13) and property correlation (17) are used.

III Steady state heat transport. The same equations as in model II are used, the energy storage term in eqn. (6) is set to zero.

3.2.2 Spatial resolution of transport equations

The spatial resolution of the partial differential equations of heat and mass transport are implemented in model I applying a finite volume method [12] for a flat plate geometry. The number of nodes is kept constant throughout the computational procedure, the moving grid therefore requires the inclusion of convective terms in the heat and mass balances which are experessed using an upwind scheme. A spatial discretization of 10 segments seems to give a satisfactory accuracy and was used in all results presented further below. The frost properties on the right hand side of equations (4) and (3) representing the inverse of the transport resistances are then defined at the boundary of two neighboring finite volumes. In case they are not constant in the spatial domain, they are determined using the harmonic mean of the terms computed for the two neighboring cells. This corresponds to finite resistances connected in series.

Combining wall and frost layer in one component is advantageous if the model should also be capable of simulating situations, when no frost layer is present due to a surface temperature higher than the triple or the dew point. In this case the proposed equation system would become singular. Including the thermal resistance of the frost in the energy balance of the first wall element until a certain frost thickness is reached makes it possible to determine the onset of frost formation by boundary conditions. The internal temperatures are set to constant during this period and are reinitialized using the `reinit` operator as soon as a threshold value for the frost layer thickness is reached. A linear distribution of the difference between wall and surface temperatures is used as start values. This approach simply neglects the energy storage capacity of the frost layer in the initial growth period. The frost porosity also remains constant during this time. The intial frost density is assumed to be $\bar{\rho}_{f,0} = 25\ \mathrm{kg/m^3}$ as suggested by [5].
Both, wall and frost layer are also discretized in air flow direction without any interdependence of neighboring cells in this dimension.

3.3 Air - frost/wall interface

When the surface temperature is above the triple point and below the dew point of the air flow, water condenses at the cold surface and is assumed to leave the system immediately. The liquid water volume is therefore not considered. The model does not include situations of water condensation on a present frost surface. The liquid would soak into the porous medium, its distribution would be very hard to predict. The connector variables required to combine the two components, airflow and frosted wall, are:

```
connector FrostPort
    SI.HeatFlowRate Q_flow "Sensible heat
    flow";
    SI.Temperature T "Surface temperature";
    SI.MassFlowRate m_flow "Water mass flow
    rate (condensing or freezing)";
    SI.MassFraction xs "Saturated absolute
    humidity at surface";
    SI.EnthalpyFlowRate H_flow "Latent heat
    flow rate";
    SI.SpecificEnthalpy h_gas "Specific
    enthalpy of vapor in bulk flow";
    SI.Velocity xf_flow "Frost layer growth
    rate";
    SI.Length x_f "Frost layer thickness";
end FrostPort;
```

The frost layer model versions I-III are organized as replaceable components in the combined aiflow/wall model. They extend from a base class which contains the parts all versions have in common, like e.g. the interface and some boundary conditions. All frost property correlations are written as functions.

4 Results and Discussion

4.1 Lumped frost layer model

Figure 3 shows the average values for frost thickness, frost density and surface temperature with respect to time and different air inlet velocities for model I. A discretization of 8 segments was chosen for the airflow dimension. If the timescale of frost growth is of primary interest the steady state model (model III) gives results similar to model II and even on a shorter timescale the heat capacity of the frost layer may be negligible. However, introducing additional numerical states may be advantageous in a more complex application to break down systems of nonlinear equations.

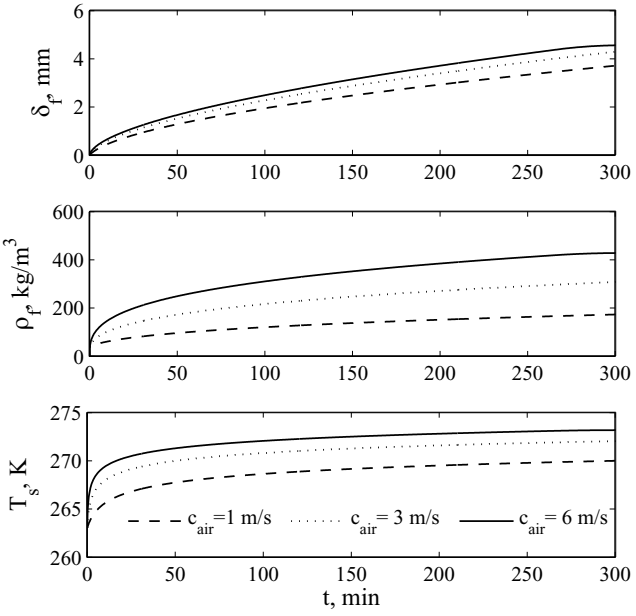

Figure 3: Frost thickness δ_f, mean frost density $\bar{\rho}_f$ and surface temperature T_s at different air inlet velocities. T_b=293K, $A_{channel,0} = 40cm^2$, T_w=263K, φ_{air}=42 %.

An increasing air flow rate leads to a higher frost deposition rate due to an increased heat and mass transfer. This creates a higher thermal resistance leading to a greater surface temperature. At the same time the density of the frost layer increases with a rising sur-

face temperature according to the used correlation for the surface density (eq. 13) which in turn reduces the thermal resistance of the total frost layer. The total thermal resistance responsible for the thermal behavior of the frosted heat exchanger surface is therefore a result of the counteracting effects of densification and frost growth.

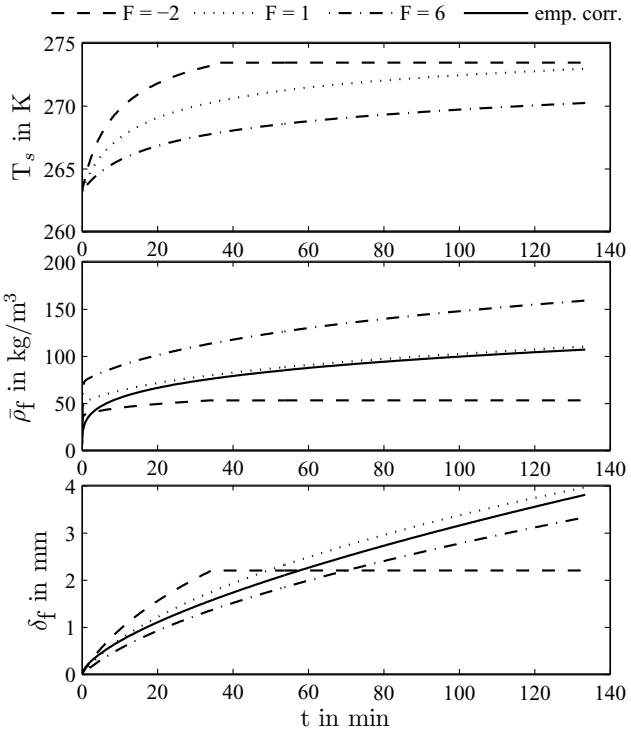

Figure 4: Surface temperature T_s, frost density $\bar{\rho}_f$ and frost layer thickness δ_f at a distance of y = 0.5 m from the leading edge over time with the diffusion enhancement factor F as a parameter. Boundary conditions: v_{air} = 2.5 m/s, T_{air} = 283K, T_w = 263K, X = 0.006 kg/kg.

4.2 Distributed frost layer model

The distributed frost layer model provides a spatial resolution of frost density with frost layer height which makes it possible to compute the local thermal resistance in the frost. However, because measurement data of these variations are scarce, the overall values of frost thickness and average frost density will be further discussed. Mao *et al.* conducted a wide range of measurements under various conditions with an airflow channel (300 mm wide and 20 mm high) that contained one cooled surface. They derived empirical correlations from their results (with a root mean square error of 0.22 for density and frost height), which are used in this work to adapt the diffusion enhancement factor F in (25). Figure 4 presents simulation results from the distributed model for different values of F.
It can be seen that frost growth and density development are strongly influenced by its value. Unfortunately Mao *et al.* did not measure the frost surface temperature, but assumed it always to be equal to 0 °C, while the model presented here does not account for melting water permeating the frost which would occur under those circumstances. Instead the frost layer growth stops as soon as the triple point temperature is reached as can be observed at t = 35 min for F = -2 caused by the low water diffusion resulting in a larger frost thickness, higher porosity and large thermal resistance of the material.

4.3 Model comparison

A comparison of model I (distributed) and model II (lumped) is given together with results from empirical correlations found by Mao *et al.* for their experimental data in figure 5 for different wall surface temperatures. The frost thickness computed with the lumped model is in good agreement with the values obtained from the empirical correlations. The average density is larger than that computed using the empirical correlation in all lumped model cases. This would also lead to a thermal resistance predicted too low. However, the deviation from the given error interval of the empirical correlation is not very large. The distributed model shows a close agreement with the empirical correlations for both, frost thickness and average density, the diffusion factor F was set to 0, 3 and 8, respectively with rising wall temperature to give a good fit. A trend towards an increasing enhancement of the diffusion factor with rising plate temperatures in a non-linear way is also reported by [6]. However, the exact values may not be transferable to different boundary conditions.
A simular trend on the average frost density can be observed with the lumped model which relates the surface density to the surface temperature. Since density has a major impact on all frost properties including the thermal conductivity its correct determination seems important. However, in both approaches some assumptions were made that strongly influence the development of frost density with time. In the distributed approach a zero density gradient is applied at the surface which is similar to the approach in [6], while correlation (13) is used for the lumped model. But it is believed that the actual structure and at the same time the density of the new frost depositing at the surface may actually differ from these assumptions.

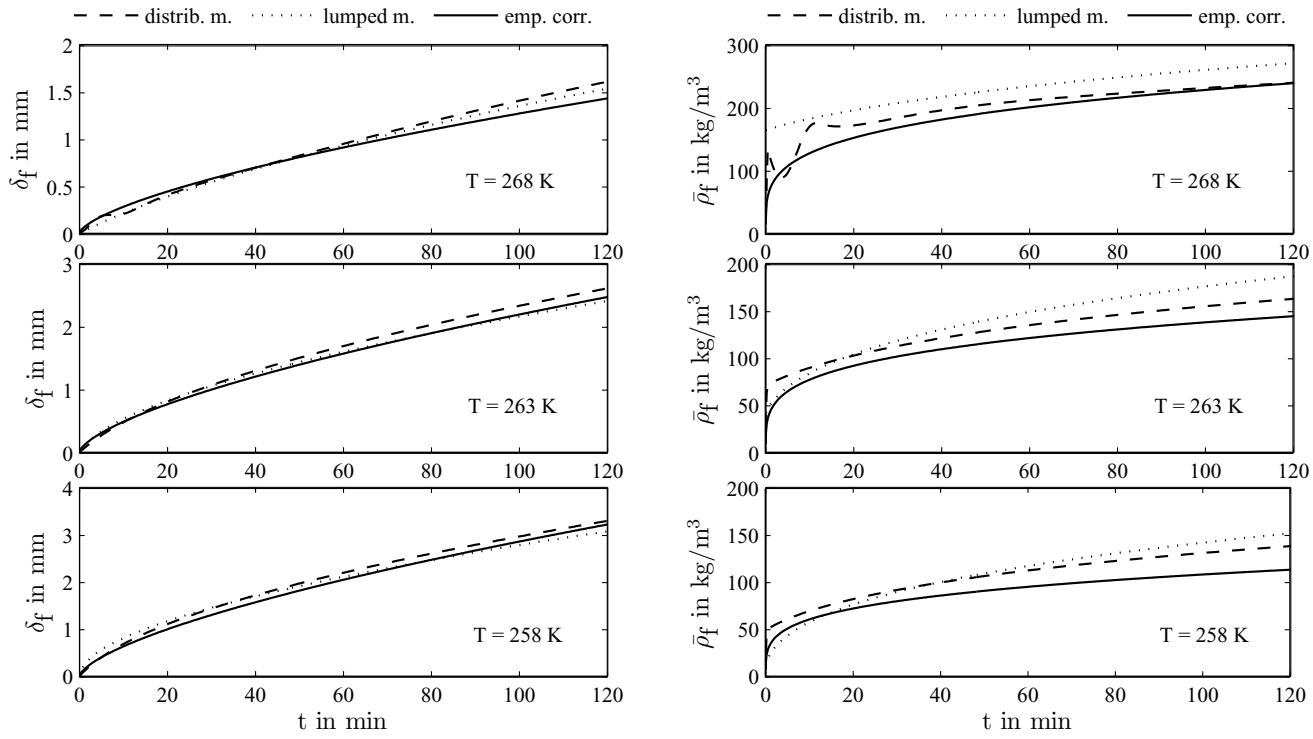

Figure 5: Frost layer thickness δ_f and average frost density $\bar{\rho}_f$over time for the lumped and the distributed model and an empirical correlation from [13]. Boundary conditions: v_{air} = 2.5 m/s, T_{air} = 291 K, X = 0.006 kg/kg, y = 0.5 m.

5 Conclusion

Resolving heat and mass transport phenomena in the spatial domain of the frost layer as it is done in model I gives only higher accuracy in predicting frost growth and average density if information on the diffusion enhancement factor F is present. The simple lumped approach (model II) is suitable to predict trends of frost formation with respect to variable boundary conditions, such as air and wall temperature, humidity and air velocity. A surprisingly good agreement is obtained for the predicted frost thickness when compared to an empirical correlation. More accurate absolute values of density and thermal resistance with regard to operating time may perhaps be obtained with a refinement of the model in terms of densification of the frost layer with time and surface density of the deposit. In addition more empirical data is required, especially in terms of the frost surface temperature, to validate the model in a wide operating range.

Modeling the frost formation process correctly provides information on the amount of frost and its ice fraction at the start of the defrost process, which gives an idea of the minimum energy required for a complete defrost. Further work is needed to describe the defrost process with time depending on the chosen strategy. The most common method of heating the solid wall material using hot gas or electrical current poses the problem of predicting the detachment of the frost layer from the wall and the associated heat transport through gaps filled with liquid water or air. In addition, heat transfer to the surrounding air by natural convection must be taken into account if the air supply is stopped during this period.

References

[1] Xia, Y., Hrnjak, P. S. and Jacobi A. M, Air-side thermal hydraulic performance of louvered-fin, flat-tube heat exchangers with sequential frost-growth cycles. *ASHRAE Transactions*, 2005, **111**, 487-495.

[2] O'Neal, D. L. and Tree D. R., A review of frost formation in simple geometries. *ASHRAE Transactions*, 1992, **98**(Part 2), 65-78.

[3] Hoffenbecker, N., Klein, S.A. and Reindl, D.T., Hot gas defrost model development and validation. *International Journal of Refrigeration*, 2005, **28**, 605-615.

[4] Sanders, C. T., Frost Formation: The influence of frost formation and defrosting on the performance of air coolers. PhD thesis, Delft University of Technology, Delft, 1974.

[5] Le Gall, R., Grillot, J. M. and Jallut, C., Modelling of frost growth and densification. *International Journal of Heat and Mass Transfer*, 1997, **40**, 3177-3187.

[6] Tao, Y. X., Besant, R., W. and Rezkallah, K. S. A mathematical model for predicting the densification and growth of frost on a flat plate. *International Journal of Heat and Mass Transfer*, 1993, **36**, 353-363.

[7] Hayashi Y., Aoki, A., Adachi, S. and Hori, K., Study of frost properties correlating with frost formation types. *Jornal of Heat Transfer*, 1977, **99**, 239-245.

[8] Baehr, H. D., Stephan, K., *Heat and Mass Transfer*. 2nd Ed., Springer Verlag, Berlin, 2006.

[9] Hayashi Y., Aoki, A. and Yuhara, H., Study of frost formation based on a theoretical model of the frost layer. Heat Transfer - Japanese Research, 1977, **6**, 79-94.

[10] Yonko, J. D. and Sepsy, C. F., An investigation of the thermal conductivity of frost while forming on a flat horizontal plate. *ASHRAE Transactions*, 1967, **73**, 1.1-1.11.

[11] Yun, R., Kim, Y. and Min, M., Modeling of frost growth and frost properties with airflow over a flat plate. *International Journal of Refrigeration*, 2002, **25**, 362-371.

[12] Patankar, S. V., *Numerical Heat Transfer and Fluid Flow*. Hemisphere Publ. Co., New York, 1980.

[13] Mao, Y., Besant, R.W., Rezkalla, K.S., Measurement and correlations of frost properties with airflowover a flat plate. *ASHRAE Transactions*, 1992, **1**, 65-78.